

Surface-Wave Control Technique for Mutual Coupling Mitigation in Array Antenna

A. Askarian¹, Student Member, IEEE, J. Yao, Fellow, IEEE, Z. Lu², Member, IEEE, and K. Wu¹, Fellow, IEEE

Abstract—We propose and investigate an easy technique to mitigate the mutual coupling of integrated antenna elements caused by surface waves in a high-permittivity grounded dielectric substrate, which can be deployed for high-density integration of antenna and front end on a substrate. Two approaches are examined to realize the proposed concept: 1) the removal of the ground plane between two collinear antennas and a series of uniform corrugations are introduced at the edges of the remaining parts to create a transition region between grounded and ungrounded regions and to form a sort of transversal surface waveguide and 2) to partially remove the ground plane with long, longitudinal, and closely spaced slots etched over the ground plane to offset the inductivity of the ground plane. Simulation and measurement results on an example based on two 25-GHz patch antennas show reductions in the mutual coupling of around 9 dB and improvement in broadside radiation pattern by 4 dBi.

Index Terms—Antenna array, antenna in package (AiP), millimeter-wave (mmW) integrated circuit, surface wave, surface waveguide.

I. INTRODUCTION

MUTUAL coupling in antenna array is attributed to two substantial effects.

- 1) *Space Waves*: When two antennas are in close vicinity (order of a quarter wavelength or less) in the H-plane, this mutual coupling is mostly related to near-field effects.
- 2) *Surface Waves*: In a high-permittivity material with a larger distance (order of a half-wavelength or more) especially over the E-plane, the contribution of surface waves in mutual coupling outweighs the near-field effects. Some papers in this connection [1]–[6] employed low-permittivity materials in which antennas either are arranged in close vicinity in the H-plane or operate at a very low frequency. In either case, the mutual coupling is mainly governed by the near fields.

Attempts have been made for suppressing or diminishing the effect of surface waves [7]–[23]. The electromagnetic

Manuscript received September 29, 2021; revised November 30, 2021; accepted December 26, 2021. Date of publication January 12, 2022; date of current version June 7, 2022. (Corresponding author: Amirhossein Askarian.)

Amirhossein Askarian and K. Wu are with the Poly-Grames Research Center, Polytechnique Montreal, Montreal, QC H3T 1J4, Canada (e-mail: a.askarian@polymtl.ca; ke.wu@polymtl.ca).

J. Yao is with the School of Electrical Engineering and Computer Science, University of Ottawa, Ottawa, ON K1N 6N5, Canada (e-mail: jpyao@uottawa.ca).

Z. Lu is with the Advanced Electronics and Photonics Research Center, National Research Council Canada (NRC), Ottawa, ON K1A 0R6, Canada (e-mail: zhenguo.lu@nrc-cnrc.gc.ca).

Color versions of one or more figures in this letter are available at <https://doi.org/10.1109/LMWC.2021.3139196>.

Digital Object Identifier 10.1109/LMWC.2021.3139196

bandgap (EBG) technique shows a great capability to alleviate the propagation of surface waves partially or completely in a specific direction or even in an isotropic manner. It can be realized with either a periodically loaded substrate with drilled holes to form a honeycomb or triangular lattice or periodically etched patterns in the ground plane [7]. In addition, it can be realized by periodic patches with a central metalized via that forms a PMC-like surface [8]–[11]. However, the realization of a proper bandgap takes up a large area and requires substrate drilling and perforation. A substrate perforation technique was introduced to create an effective permittivity of dielectric slab [12]. Micromachining is another technique that is usually employed for AoC to enhance radiation efficiency and reduce the amount of power coupled to surface waves [13]–[19]. The soft and hard surface (SHS) technique, either in a trench or via hole configuration, can also alleviate the propagation of surface waves to some extent [20]–[23]. Although these techniques are still applicable and valuable, in this letter, we present a small-footprint, low-cost, and easy-to-adopt surface-wave control technique for high- k material-based integrated antenna array in which no laser drilling or metallization is required.

II. THEORY AND METHODOLOGIES

To characterize surface-wave modes in a dielectric slab, the well-established odd–even mode analysis can be applied to develop two sets of even and odd equations for TM and TE waves. A general solution of electromagnetic (EM) analysis in a dielectric slab includes a linear combination of both odd and even modes. However, in a grounded dielectric, due to boundary conditions, the TE waves only include odd modes, while TM waves hold even modes [24].

Fig. 1 shows the dispersion diagram of surface-wave modes with propagation constant β for a grounded RT/Duroid 6010 ($\epsilon_r = 10.2$ and thickness of 25 mil), which is not only used for mimicking a semiconductor substrate but also for experimental validations in this work. As indicated, the cutoff frequency of TE_1 is around 39 GHz ($d/\lambda_0 \approx 0.09$); therefore, only TM_0 mode of surface waves is excited in our desired frequency range (24–32 GHz).

As is well known, TM modes propagate on an inductive surface, while TE modes require a capacitive impedance surface for propagation. To reduce the surface inductance for disrupting the propagation of TM_0 mode, we remove the ground plane between the two collinear antennas. To investigate the surface impedance of the created ungrounded region, we evaluate the dispersion diagram of surface waves.

A general and accurate EM solution for the ungrounded dielectric slab, including a linear combination of both odd

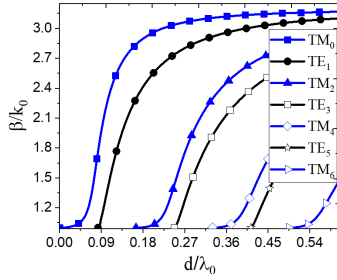


Fig. 1. Normalized dispersion diagram of surface-wave modes for grounded RT/Druid 6010 with thickness of “d.”

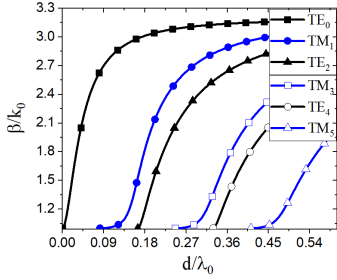


Fig. 2. Normalized dispersion diagram of surface-wave modes for ungrounded RT/Druid 6010 with thickness of “d.”

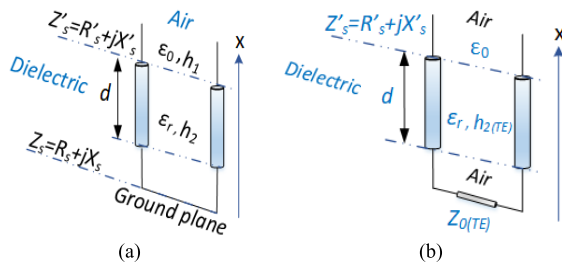


Fig. 3. (a) TEN model for grounded dielectric with thickness of “d.” h_1 and h_2 are propagation constants of surface waves in air and dielectric, respectively, along the x -axis, z_s is the surface impedance of ground plane, and z'_s is the surface impedance of air–dielectric boundary. (b) TEN model for ungrounded dielectric loaded with air impedance (Z_{0TE} is the air impedance for TE mode).

and even modes of TM and TE waves, calls for a full-wave simulation. However, due to employing a high-permittivity dielectric slab ($\epsilon_r \gg \epsilon_r^{\text{air}} = 1$), the ungrounded surfaces can be considered as PMC-like surfaces. Using this approximate yet acceptable condition, we estimate the dispersion diagram for an ungrounded dielectric slab as shown in Fig. 2, which includes solely even TE modes and odd TM modes. Obviously, in the desired frequency spectrum ($d/\lambda_0 < 0.1$), only the TE_0 mode propagates along the substrate.

Having employed the transverse equivalent network (TEN) model (Fig. 3) along with the TL theory according to (1) (where $\beta^2 + h_2^2 = \epsilon_r k_0^2$, η_0 is the intrinsic impedance of air, σ is the conductivity of copper, k_0 is the free-space wavenumber, $Z_2^{\text{TM}_n} = \eta_0 h_2^{\text{TM}_n} / \epsilon_r k_0$, $Z_2^{\text{TE}_m} = \eta_0 k_0 / h_2^{\text{TE}_m}$, and $Z_s = R_s + jX_s = (1 + j)(\eta_0 k_0)^{1/2} / 2\sigma$; $n, m = 0, 1, 2, \dots$), we calculated the normalized surface reactance (X'_s / η_0) of the air–dielectric interface for both grounded and ungrounded dielectrics as shown in Fig. 4(a)

$$Z'_s = Z_2^{\text{TM}_n/\text{TE}_m} \frac{Z_{\text{load}} + j Z_2^{\text{TM}_n/\text{TE}_m} \tan\left(2\pi \frac{h_2^{\text{TM}_n/\text{TE}_m}}{k_0} \frac{d}{\lambda_0}\right)}{Z_2^{\text{TM}_n/\text{TE}_m} + j Z_{\text{load}} \tan\left(2\pi \frac{h_2^{\text{TM}_n/\text{TE}_m}}{k_0} \frac{d}{\lambda_0}\right)}. \quad (1)$$

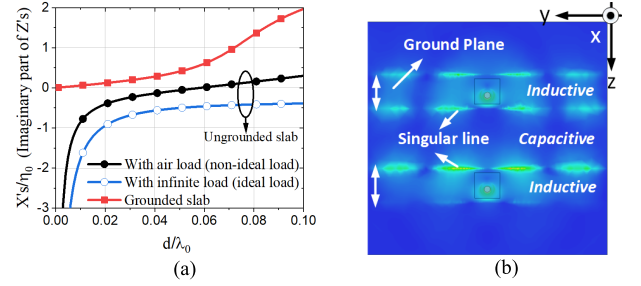


Fig. 4. (a) Normalized surface reactance for both grounded and ungrounded dielectric slabs with thickness of “d.” (b) Magnetic field distribution for the antenna array with disjoint ground planes.

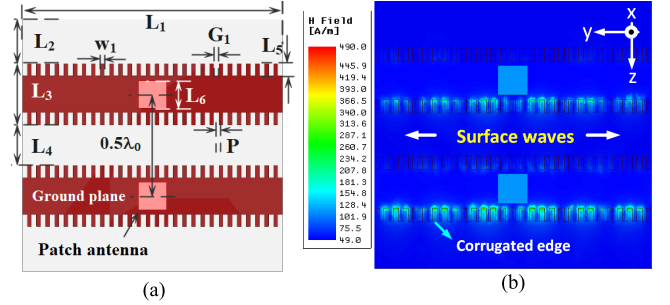


Fig. 5. (a) Geometry of collinear antenna array with corrugated ground plane, $L_1 = 12.82$, $L_2 = 2.1$, $L_3 = 3.2$, $L_4 = 1.8$, $L_5 = 0.7$, $L_6 = 1.36$, $W_1 = 0.2$, $G_1 = 0.25$, and $P = 0.45$ (all dimensions are in millimeter). (b) Magnetic field distribution of corrugated ground plane.

We consider two scenarios for developing the TEN model for the ungrounded region: 1) an open-ended TL corresponding to PMC surface (ideal load) and 2) a TL loaded with air impedance (nonideal load), as shown in Fig. 3(b). As shown in Fig. 4(a), the surface impedance is capacitive for the ideal load (infinite load) and it becomes somewhat inductive for the nonideal load (air impedance) as d/λ_0 approaches 0.1, while the grounded region is inductive over the entire range. In both scenarios, alteration in surface impedance is pronounced between the grounded and ungrounded regions.

This step change in surface impedance creates a narrow discontinuity/singular region between grounded and ungrounded parts, as shown in Fig. 4(b). The trapped TM_0 and TE_0 surface waves on either side of this singular line create standing waves, which not only leads to impedance mismatch in antennas but also increases the back radiations, as shown in Fig. 7(b).

A. Ground Plane With Corrugated Edges

By introducing a series of tiny corrugations in the ground plane’s edges [25]–[27], as suggested in Fig. 5(a), back radiations are alleviated to a tangible extent, as shown in Fig. 7(b). In this case, surface waves will be guided to the transverse direction [y -axis in Fig. 5(b)] through the corrugated edges. Fig. 5(b) shows the magnetic field distribution in the corrugated ground plane, signifying that the corrugated parts act as transversal surface waveguides.

According to the simulation results shown in Fig. 7(a), this technique with corrugation length around a quarter guided wavelength sets to reduce mutual coupling by 9 dB. The minimum corrugation pitch “ P ” and width “ W_1 ” (which are also optimum values [27]) were restricted by our PCB fabrication process in the Poly-Grames Research Center.

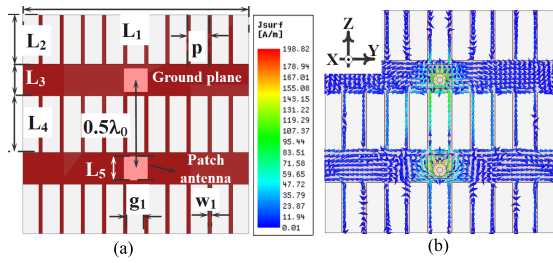


Fig. 6. (a) Geometry of collinear antenna array with slotted ground plane, $L_1 = 12.82$, $L_2 = 2.8$, $L_3 = 1.8$, $L_4 = 3.2$, $L_5 = 1.36$, $W_1 = 0.2$, $g_1 = 1$, and $p = 1.2$ (all dimensions are in millimeter). (b) Current distribution on slotted ground plane.

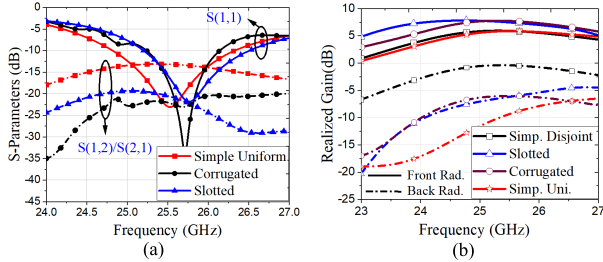


Fig. 7. (a) Simulated S -parameters for antenna array with simple uniform, corrugated, and slotted ground planes [according to dimensions mentioned in Figs. 5(a) and 6(a)]. (b) Simulated front and back radiations for antenna with simple uniform, disjoint without corrugation, corrugated edges, and slotted ground planes.

B. Longitudinal Parallel Slots in Ground Plane

In some applications such as reconfigurable antenna array and AiA, the ground plane is also employed as a monolithic dc conductor. Therefore, we extend the corrugation region to form parallel and closely spaced longitudinal slots (slotted and connected ground plane) between two collinear antennas [Fig. 6(a)]. These slots abate the inductivity of the ground plane, hence, in the air–dielectric surface. In addition, due to the resonance length of the narrow strips and as the current distribution reveals in Fig. 6(b), each strip would act as a local radiator excited by the TM_z mode of the surface wave. The simulated scattering parameters in Fig. 7(a) indicate that this technique can mitigate the mutual coupling by 9 dB.

In fact, the proposed techniques can control excited surface waves and make use of them to the broadside radiation through slotted and corrugated regions, as shown in Fig. 7.

III. FABRICATION AND MEASUREMENT

To validate the analysis and the theoretical results, we fabricated three experimental prototypes, including antenna arrays with the uniform (as our reference), corrugated edges, and the slotted ground planes on RT/Duroid 6010 with a thickness of 25 mil, as shown in Fig. 8(a) and (b). To control the surface waves, we added another layer of RT/Duroid 5880 substrate with low relative permittivity of 2.2 and thickness of 20 mil and extended it to install the end-launch connectors. Microstrip lines in the bottom layer (RT/Duroid 5880) were connected to the patch antennas on the top layer through metallic pins with a diameter of 15 mil.

Experimental results in Fig. 8(c) show a reduction of 8 and 11 dB in mutual coupling in the antennas with the slotted and corrugated ground planes, respectively. Fig. 9 shows the normalized radiation patterns for the three fabricated antennas. Compared to the antenna with a uniform ground plane,

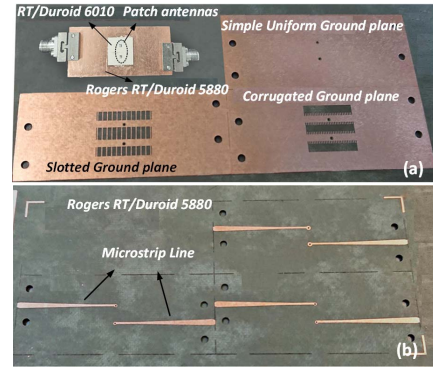


Fig. 8. (a) Top and (b) bottom views of substrates and an assembled prototype equipped with two end-launch connectors (inset). (c) Comparison between measured S -parameters.

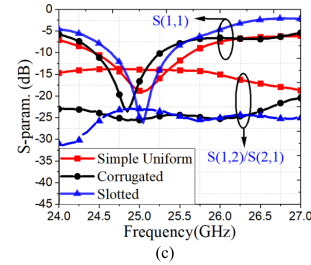


Fig. 9. Measured normalized E-plane radiation patterns of three prototypes.

both the corrugated edges and slotted ground planes show significant improvements in broadside radiation by 4 dB since the radiation pattern in a simple uniform ground plane has a maximum at -75° . Furthermore, the antenna with uniform ground plane shows a null at -30° , which is diminished in the slotted antenna and almost disappears in the corrugated ground planes. This null is formed by the diffraction of the guided surface waves from the truncated edges of the ground plane and its destructive interactions with the radiated space waves at a specific angle.

IV. CONCLUSION

We proposed a compact and easy-to-realize technique for controlling surface waves in a grounded dielectric of large relative permittivity. In this research, we investigated the effect of alteration surface impedance by removing the ground plane between two antennas and disrupting the propagation of surface waves. This methodology, related to an example based on two 25-GHz patch antennas, alleviates mutual coupling by around 9 dB and improves broadside gain by 4 dB. The presented technique outperforms other methodologies in terms of the combined advantages of small footprint, low profile, and concurrent appreciable improvement in both mutual coupling and radiation pattern. Considering all the above-mentioned advantages on a high- k substrate, we believe that it can be easily applied to the design scenarios of an integrated antenna array.

REFERENCES

- [1] F. Liu, J. Guo, L. Zhao, G.-L. Huang, Y. Li, and Y. Yin, "Ceramic superstrate-based decoupling method for two closely packed antennas with cross-polarization suppression," *IEEE Trans. Antennas Propag.*, vol. 69, no. 3, pp. 1751–1756, Mar. 2021.
- [2] F. Liu, J. Guo, L. Zhao, G.-L. Huang, Y. Li, and Y. Yin, "Dual-band metasurface-based decoupling method for two closely packed dual-band antennas," *IEEE Trans. Antennas Propag.*, vol. 68, no. 1, pp. 552–557, Jan. 2020.
- [3] X. Shen, Y. Liu, L. Zhao, G.-L. Huang, X. Shi, and Q. Huang, "A miniaturized microstrip antenna array at 5G millimeter-wave band," *IEEE Antennas Wireless Propag. Lett.*, vol. 18, no. 8, pp. 1671–1675, Aug. 2019.
- [4] S. Zhu, H. Liu, Z. Chen, and P. Wen, "A compact gain-enhanced Vivaldi antenna array with suppressed mutual coupling for 5G mmWave application," *IEEE Antennas Wireless Propag. Lett.*, vol. 17, no. 5, pp. 776–779, Mar. 2018.
- [5] A. Kianinejad, Z. N. Chen, and C.-W. Qiu, "Full modeling, loss reduction, and mutual coupling control of spoof surface plasmon-based meander slow wave transmission lines," *IEEE Trans. Microw. Theory Techn.*, vol. 66, no. 8, pp. 3764–3772, Aug. 2018.
- [6] Y.-X. Guo, K.-M. Luk, and K.-W. Leung, "Mutual coupling between millimeter-wave dielectric-resonator antennas," *IEEE Trans. Microw. Theory Techn.*, vol. 47, no. 11, pp. 2164–2166, Nov. 1999.
- [7] R. Gonzalo, P. de Maagt, and M. Sorolla, "Enhanced patch-antenna performance by suppressing surface waves using photonic-bandgap substrates," *IEEE Trans. Microw. Theory Techn.*, vol. 47, no. 11, pp. 2131–2138, Nov. 1999.
- [8] T. Kamgaing and O. M. Ramahi, "Multiband electromagnetic-bandgap structures for applications in small form-factor multichip module packages," *IEEE Trans. Microw. Theory Techn.*, vol. 56, no. 10, pp. 2293–2300, Oct. 2008.
- [9] J.-W. Jeong and J.-S. Park, "A microcontroller unit-based electromagnetic bandgap control scheme: Application for enhancing isolation in an antenna array and the EMI scanner system speed thereof," *IEEE Trans. Microw. Theory Techn.*, vol. 68, no. 11, pp. 4536–4553, Nov. 2020.
- [10] S. D. Rogers, "Electromagnetic-bandgap layers for broad-band suppression of TEM modes in power planes," *IEEE Trans. Microw. Theory Techn.*, vol. 53, no. 8, pp. 2495–2505, Aug. 2005.
- [11] J. Park, A. C. W. Lu, K. M. Chua, L. L. Wai, J. Lee, and J. Kim, "Double-stacked EBG structure for wideband suppression of simultaneous switching noise in LTCC-based SiP applications," *IEEE Micro. Wireless Compon. Lett.*, vol. 16, no. 9, pp. 481–483, Sep. 2006.
- [12] J. S. Colburn and Y. Rahmat-Samii, "Patch antennas on externally perforated high dielectric constant substrates," *IEEE Trans. Antennas Propag.*, vol. 47, no. 12, pp. 1785–1794, Dec. 1999.
- [13] J.-G. Yook and L. P. B. Katehi, "Micromachined microstrip patch antenna with controlled mutual coupling and surface waves," *IEEE Trans. Antennas Propag.*, vol. 49, no. 9, pp. 1282–1289, Sep. 2001.
- [14] J.-C. Langer, J. Zou, C. Liu, and J. T. Bernhard, "Micromachined reconfigurable out-of-plane microstrip patch antenna using plastic deformation magnetic actuation," *IEEE Microw. Wireless Compon. Lett.*, vol. 13, no. 3, pp. 120–122, Mar. 2003.
- [15] H. Zhu, X. Li, W. Feng, J. Xiao, and J. Zhang, "A compact 267 GHz shorted annular ring antenna with surface wave suppression in 130 nm SiGe BiCMOS," *IEEE Antennas Wireless Propag. Lett.*, vol. 17, no. 5, pp. 760–763, May 2018.
- [16] A. R. Alajmi and M. A. Saed, "A pin-loaded microstrip patch antenna with the ability to suppress surface wave excitation," *Prog. Electromagn. Res. C*, vol. 62, pp. 131–137, 2016.
- [17] I. Papapolymerou, R. F. Drayton, and L. P. B. Katehi, "Surface wave mode reduction for rectangular microstrip antennas," in *Proc. IEEE Antennas Propag. Soc. Int. Symp.*, Newport Beach, CA, USA, vol. 3, Jun. 1995, pp. 1494–1497.
- [18] D. R. Jackson, J. T. Williams, A. K. Bhattacharyya, R. L. Smith, S. J. Buchheit, and S. A. Long, "Microstrip patch designs that do not excite surface waves," *IEEE Trans. Antennas Propag.*, vol. 41, no. 8, pp. 1026–1037, Aug. 1993.
- [19] M. A. Khayat, J. T. Williams, D. R. Jackson, and S. A. Long, "Mutual coupling between reduced surface-wave microstrip antennas," *IEEE Trans. Antennas Propag.*, vol. 48, no. 10, pp. 1581–1593, Oct. 2000.
- [20] R. Li, G. DeJean, M. M. Tentzeris, J. Papapolymerou, and J. Laskar, "FDTD analysis of patch antennas on high dielectric-constant substrates surrounded by a soft-and-hard surface," *IEEE Trans. Magn.*, vol. 40, no. 2, pp. 1444–1447, Mar. 2004.
- [21] D. Li and K. Wu, "Geometric characteristics, physical mechanism, and electrical analysis of quasi-TEM waveguides with dipole-FSS walls," in *IEEE MTT-S Int. Microw. Symp. Dig.*, May 2010, pp. 17–20.
- [22] D. Li, N. K. Mallat, and K. Wu, "Quasi-TEM rectangular waveguides with frequency selective surface walls—Part I: Electrical properties and geometrical characteristics," *Int. J. Numer. Model., Electron. Netw., Devices Fields*, vol. 27, no. 2, pp. 334–352, Mar. 2014.
- [23] M. Belaid and K. Wu, "Spatial power amplifier using a passive and active TEM waveguide concept," *IEEE Trans. Microw. Theory Techn.*, vol. 51, no. 3, pp. 684–689, Mar. 2003.
- [24] R. E. Collin and H. Chang, *Field Theory of Guided Waves*, 2nd ed. New York, NY, USA: Wiley, 1990.
- [25] Y. Liang, H. Yu, H. C. Zhang, C. Yang, and T. J. Cui, "On-chip sub-terahertz surface plasmon polariton transmission lines in CMOS," *Sci. Rep.*, vol. 5, no. 1, Oct. 2015, Art. no. 14853.
- [26] Y. Liang, H. Yu, G. Feng, A. A. A. Apriyana, X. Fu, and T. J. Cui, "An energy-efficient and low-crosstalk sub-THz I/O by surface plasmonic polariton interconnect in CMOS," *IEEE Trans. Microw. Theory Techn.*, vol. 65, no. 8, pp. 2762–2774, Aug. 2017.
- [27] L. Ji, X.-C. Li, and J.-F. Mao, "Half-mode substrate integrated waveguide dispersion tailoring using 2.5-D spoof surface plasmon polaritons structure," *IEEE Trans. Microw. Theory Techn.*, vol. 68, no. 7, pp. 2539–2550, Jul. 2020.